^{99m}Tc-Annexin V Imaging for In Vivo Detection of Atherosclerotic Lesions in Porcine Coronary Arteries

Lynne L. Johnson, MD[1]; Lorraine Schofield, BS[1]; Tammy Donahay, BS[1]; Navneet Narula, MD[2]; and Jagat Narula, MD, PhD[2]

[1]*Rhode Island Hospital, Providence, Rhode Island; and* [2]*University of California, Irvine, California*

We used a model of porcine coronary atherosclerosis characterized by smooth muscle cell apoptosis to test the hypothesis that apoptosis of cells in the vascular wall of coronary arteries can be detected on SPECT images using a technetium-labeled radiotracer that targets apoptosis. **Methods:** Eleven juvenile male swine received a high-fat diet combined with injury to 22 coronary vessels. After 51 ± 9 d (mean ± SD), the animals underwent coronary angiography, were injected with 403.3 ± 48.1 MBq of ^{99m}Tc-annexin V, underwent SPECT, and were sacrificed. The coronary arteries underwent autoradiography and well counting, and immunostaining was performed for α-actin, caspase, and macrophages. **Results:** Atherosclerotic lesions were predominantly of American Heart Association class II. Thirteen of the 22 injured vessels showed focal uptake of ^{99m}Tc-annexin V in vivo (scan positive), and 9 injured vessels and all control vessels showed no focal uptake (scan negative). The count ratios of the injured vessels to the control vessels were 2.38 ± 0.61 for scan-positive vessels and 1.27 ± 0.23 for scan-negative vessels ($P < 0.001$). The percentages of injected dose for the scan-positive and scan-negative vessels were 1.73 ± 0.83 × 10^{-3} and 0.68 ± 0.20 × 10^{-3}, respectively ($P < 0.001$). Immunohistopathologic examination found that the cells undergoing apoptosis were smooth muscle cells. The apoptotic index (caspase-positive cells to total cells) was 63% ± 7% for scan-positive vessels and 16% ± 10% for scan-negative vessels ($P < 0.001$). Both the count ratio of injured vessels to control vessels and the percentage injected dose correlated significantly with death rate by regression analysis. **Conclusion:** Annexin is a noninvasive method to identify plaque apoptosis in the coronary vessels.

Key Words: apoptosis; coronary atherosclerosis; annexin V

J Nucl Med 2005; 46:1186–1193

Apoptosis of both macrophages and vascular smooth muscle cells is seen in the wall of atherosclerotic vessels. Smooth muscle cells undergoing programmed death have been found predominantly in the fibrous parts of plaque, have been shown to express genes encoding for inflammatory cytokines and chemoattractant factors (*1*), and colocalize with oxidized low-density lipoprotein (*2*). Apoptosis of macrophages is found in the vulnerable plaque (*1*). Animal studies that helped elucidate the pathogenesis of atherosclerosis used a domestic swine model of hypercholesterolemia and showed both proliferation and death of smooth muscle cells in early intimal lesions (*3,4*). Compared with adjacent media, 4 times as many cells in the neointima were undergoing cell death. These studies also showed high death rates of smooth muscle cells both in lesions of the abdominal aorta and in lesions of the coronary arteries.

Phosphatidylserine is exposed on cell surfaces undergoing apoptosis. Annexin V is an endogenous protein with high affinity for phosphatidylserine bound to cell membranes. Apoptosis in vascular and myocardial lesions has been observed in both animal and human studies (*5–10*). Kolodgie et al. showed uptake of ^{99m}Tc-annexin V on in vivo γ-imaging of experimental atherosclerotic lesions of the abdominal aorta in New Zealand rabbits and localized the uptake to macrophages (*11*). The hypothesis for this present study was that apoptosis of the component cells of coronary artery plaque in a large-animal model can be detected in vivo using ^{99m}Tc-annexin V and SPECT.

MATERIALS AND METHODS

Animal Welfare

For all experiments, conditioned, castrated male juvenile swine weighing 20–30 kg were used. All experiments were performed within the National Institutes of Health guidelines for the care and use of laboratory animals and with the approval of the Rhode Island Hospital Animal Care Committee. For 1 wk before coronary artery injury, all animals received a high-fat diet. The first 8 animals received a high-fat diet plus cholic acid, and the last 3 received a specially formulated diet (TD 01076; Harlan Teklad) containing 6% cholesterol. Beginning the day before the procedure and for 7 d after the procedure, the animals received 75 mg of indomethacin in fruit juice once daily to prevent initial thrombosis at the injury site.

Received Jan. 12, 2005; revision accepted Mar. 21, 2005.

For correspondence or reprints contact: Lynne L. Johnson, MD, Columbia University Medical Center PH-10-405, New York, NY 10032.

E-mail: lj2129@columbia.edu

Instrumentation and Coronary Injury

The animals were immobilized with an intramuscular injection of tiletamine hydrochloride and zolazepam hydrochloride (Telazol; Fort Dodge Animal Health) combined with xylazine. An intramuscular injection of 0.1 mg of buprenorphine (Buprenex; Reckitt Benckiser Pharmaceuticals) per kilogram of body weight was given to provide postsurgical analgesia. An ear vein was numbed with ethyl chloride and cannulated with a 20-gauge indwelling catheter through which intravenous sodium thiopental anesthesia (Pentothal; Abbott Laboratories) was injected. After being anesthetized to a level sufficient to suppress the gag reflex, the animal was intubated. The animal was then placed on the procedure table, and the anesthesia was switched to inhaled isoflurane/N_2O. The electrocardiogram was continuously monitored. An incision was made in the neck using sterile technique, with electrocautery to minimize bleeding, and the right carotid artery was dissected free. An 8-French sheath with side arm was introduced into the carotid artery using percutaneous technique. Blood pressure and blood gas levels were monitored using the side arm. A guide catheter was inserted into the sheath and advanced into one of the coronary arteries, and angiograms were obtained using x-ray fluoroscopy. In the first experiment, endothelial injury was attempted with a guidewire. Because no detectable denudation occurred, a balloon was used for subsequent experiments. A balloon catheter was advanced into one of the coronary arteries, and the vessel was denuded and expanded. The procedure was repeated on a second coronary artery. Angiography was repeated to verify the patency of the coronary arteries. All catheters and the sheath were then removed. The carotid artery was ligated, and the neck incision was cleaned with saline and closed. The anesthesia was then discontinued, and the animal was allowed to awaken sufficiently to breathe spontaneously. The animal was then returned to the Central Research Facility, where it was housed for the remainder of the study.

Tracer Injection, Imaging, and Sacrifice

At 51 ± 7 d (mean ± SD) after injury, the animals underwent coronary angiography, tracer injection, imaging, and sacrifice. Based on the size of each animal, the maximal time was allowed for development of the lesion (*12*). Each animal was lightly sedated and intubated and then was switched from intravenous anesthesia to inhalation anesthesia. Cutdowns were performed on the right carotid artery and right internal jugular vein. Coronary angiography was performed through the carotid artery. A dose of 403.3 ± 48.1 MBq of ^{99m}Tc-annexin V was injected through an ear vein. In the first 3 experiments, frequent venous blood samples were drawn over 2 h from the right internal jugular vein and were counted to measure blood-pool clearance of the radiotracer. Serial planar imaging was performed over 2–3 h. From these data, the optimal time for imaging after tracer injection was determined. Approximately 1.5 h after injection, the animals were imaged on an Arc 3000 SPECT scanner (ADAC/Phillips) using a general all-purpose collimator and a window centered over the 140-keV photopeak of ^{99m}Tc. One animal served as a control. After undergoing the coronary artery injury and consuming the high-fat diet for 40 d, it received a 296 MBq injection of ^{99m}Tc-diethylenetriaminepentaacetic acid (DTPA) and was imaged.

After imaging was completed, each animal was euthanized and the heart rapidly excised. The coronary vessels were dissected, fixed in formalin, placed on phosphor screens for autoradiography, cut into 1-cm segments, weighed, and counted in the well counter. The heart was sliced into 1-cm sections, which were laid on the detector face and imaged. The slices were then stained with triphenyltetrazolium chloride, placed in formalin, and scanned.

Scan Interpretation

Transverse, coronal, and sagittal images were interpreted by 2 observers using triangulation display software (NC Systems). Observers were unaware of the number and location of injured vessels or the coronary angiography results. Scans were interpreted as positive if focal uptake of tracer was seen to be localized to the same region of the heart in all 3 planes. The initial reading was either positive or negative, with either 1 or 2 vessels identified. Further localization was attempted using the following scheme: Midline and anterior focal uptake was considered to be in the left anterior descending coronary artery (LAD); right and more posterior focal uptake, in the right coronary artery (RCA); and left and more posterior focal uptake, in the left circumflex coronary artery (LCX). If posterior focal uptake was identified in 2 areas, they were considered to be the RCA and the LCX.

Histopathology and Quantitative Morphometry

The coronary vessels were carefully dissected. Sections (4 μm) were cut and stained. Adjacent sections were stained for α-actin, macrophages, and caspase. Primary antibodies were used against smooth muscle α-actin (M0851; DakoCytomation), against rabbit macrophages (RAM11, M0633; DakoCytomation), and against caspase-3 (AF835; R&D Systems). Labeled polymer horseradish peroxidase secondary antibodies were used (LASAB-2 system, DakoCytomation), and the chromagen was 3,3′-diaminobenzidine. Nuclear counterstaining was done with hematoxylin (Sigma) for α-actin sections and with methyl green for caspase sections. The apoptotic index was calculated as the percentage of caspase-positive cells divided by the total cells per field.

Statistical Methods

Numeric data for the 2 groups (scan positive and scan negative) were compared using a 2-sample *t* test with equal variance. The vessel count ratios (injured-to-normal) were plotted against the apoptotic indices, and a simple linear regression was performed.

RESULTS

Coronary Vessels, Tracer Injection, and Clearance

A total of 22 vessels were injured. In 1 animal all 3 vessels were injured and a distal vessel was used as a control; in another animal only 1 vessel was injured. Therefore, there were a total of 12 control vessels. From injury to imaging, animals doubled their weights from 23 ± 2 to 50 ± 7 kg. Cholesterol values averaged 102 ± 5.7 mg/dL at baseline and 130 ± 17 mg/dL at the end of the study. In the last 3 animals, which were fed the 6% cholesterol diet, the average cholesterol value increased to 182 mg/dL. On coronary angiography, only minimal luminal irregularities were seen, and no stenotic lesion narrowed the luminal diameter by >50%.

A mean dose of 403.3 ± 48.1 MBq of ^{99m}Tc-annexin V was injected intravenously, and SPECT was performed approximately 1.5 h later. The time to imaging was based on

blood-pool clearance data obtained in the first 2 experiments. The half-lives were 6.7 min for the first component and 78.4 min for the second component. By 100 min after injection, the blood-pool activity was down to 8% of peak activity.

Scan Results

Focal uptake of ^{99m}Tc-annexin V was localized to a site of injury in 13 vessels, whereas 21 vessels were scan negative, including 9 injured vessels and the 12 control vessels (Table 1). Examples of scans read as positive and negative for focal uptake of radiotracer localized to a coronary artery are shown in Figure 1. In addition to vascular uptake of ^{99m}Tc-annexin V, focal myocardial uptake of ^{99m}Tc-annexin V was seen on in vivo images and confirmed on ex vivo images of 6 of 11 animals, corresponding to myocardial infarction by triphenyltetrazolium chloride staining as shown in Figure 2.

The mean count ratio of the injured vessels to the control vessels was 2.38 ± 0.61 for scan-positive vessels and 1.27 ± 0.23 for scan-negative vessels ($P < 0.0001$). The mean percentage injected dose was $1.73 \pm 0.83 \times 10^{-3}$ for scan-positive vessels and $0.68 \pm 0.20 \times 10^{-3}$ for scan-negative vessels ($P = 0.0001$).

Immunohistochemistry

Histopathologic examination showed that the lesions were predominantly of American Heart Association class II (Fig. 3).

The apoptosis rates ranged from 1% to 80% in injured vessel sections and from 0.7% to 8% in uninjured vessel sections. Staining of serial sections for α-actin and for macrophages showed that the cells undergoing apoptosis were smooth muscle cells (Fig. 4). No thrombi were found in any of the vessel sections. The death rate was 62.8% ± 7.2% for scan-positive injured vessels, 15.8% ± 10% for scan-negative injured vessels, and 3.7% ± 2.6% for control vessels ($P < 0.001$). Sections from scan-positive and scan-negative vessels stained for caspase are shown in Figure 5. All 12 of the scan-positive vessels had a death rate of ≥50% (Table 1). All but one of the scan-negative injured vessels had a death rate of <50%; one had a rate of 52.5%. Four scan-positive vessels had an apoptotic index of 50%–56%.

TABLE 1
Results of Scanning and Immunohistochemistry

Experiment no.	Vessel	Count ratio	Apoptosis rate (%)	In vivo scan interpretation
2	LAD	2.6	60	Positive
	RCA	2.4	61	Positive
	LCX control		Tissue lost	Negative
3	LAD	Data lost	68	Positive
	RCA		62	Positive
	LCX control		Tissue lost	Negative
4	LAD	2	56	Positive
	RCA	2	54	Positive
	LCX control		3	Negative
5	LCX	1.5	33	Negative
	RCA	1.1	30	Negative
	LAD control		6	Negative
6	LCX	1.3	20	Negative
	RCA	2	63	Positive
	LAD control		8	Negative
7	LCX	0.9	12	Negative
	RCA	1.5	16	Negative
	LAD control		6	Negative
8	RCA	2.5	68	Positive
	LCX control		15	Negative
	LAD not injected		9	Negative
9	LCX	1.5	52.5	Negative
	RCA	4	80	Positive
	LAD	2.7	Tissue lost	Positive
	Distal LAD control		0.7	Negative
10	LCX	2.1	60	Positive
	RCA	1.2	6	Negative
	LAD control		2.4	Negative
11	LAD	1.4	16	Negative
	LCX	1	1	Negative
	RCA control		1.3	Negative
12	RCA	2	50	Positive
	LCX	1.9	56	Positive
	LAD control		2	Negative

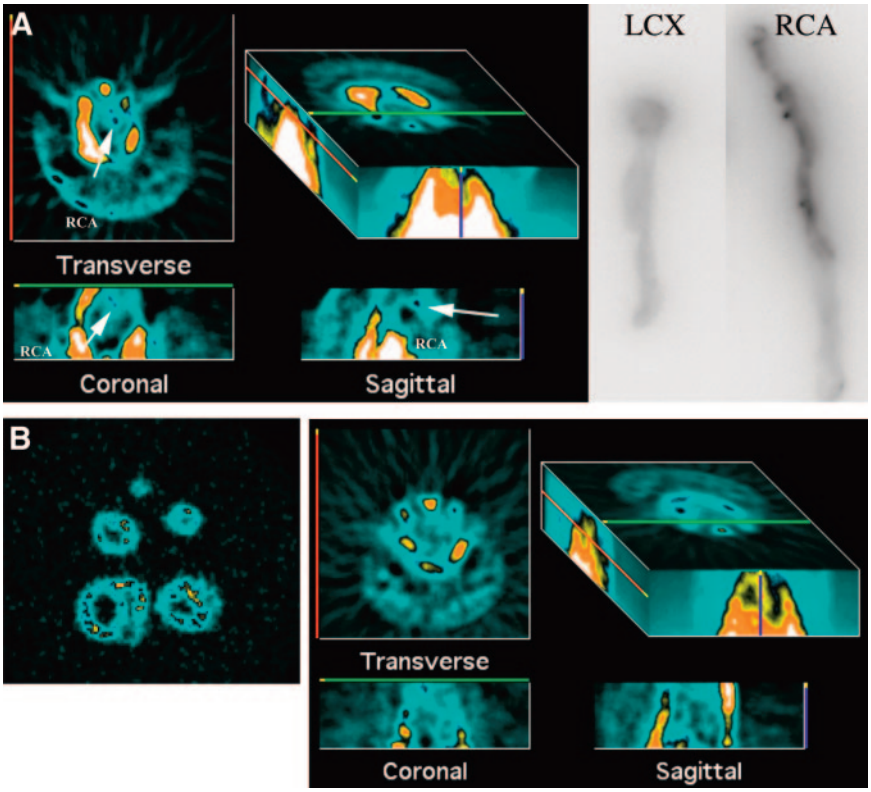

FIGURE 1. (A) Example of scan-positive vessel, with in vivo SPECT reconstructions on left and phosphor screen images on right. RCA was injured vessel, and LCX was control vessel. Phosphor screen images show tracer uptake in proximal half of RCA specimen. Transverse, coronal, and sagittal reconstructions of in vivo images show linear uptake of tracer in region of RCA. In 3-dimensional image, upper threshold is turned down to bring out any focal uptake and exaggerate bone and liver activity. (B) Example of scan-negative vessel. Myocardial slices imaged on detector are on left and in vivo SPECT reconstructions on right. Scaling is similar to that in A. No focal uptake of tracer is seen in region of heart.

The control animal injected with ^{99m}Tc-DTPA showed no focal uptake of tracer in the region of the heart but had a high apoptotic index in the LAD, as shown in Figure 6. When the apoptotic index was plotted against the ratio of counts in the injured vessel to counts in the control vessel, a significant relationship was found ($r^2 = 0.715$; $P < 0.001$). Likewise, when the apoptotic index was plotted against the percentage injected dose, a significant correlation was found ($r^2 = 0.691$; $P < 0.001$). These plots are shown in Figure 7.

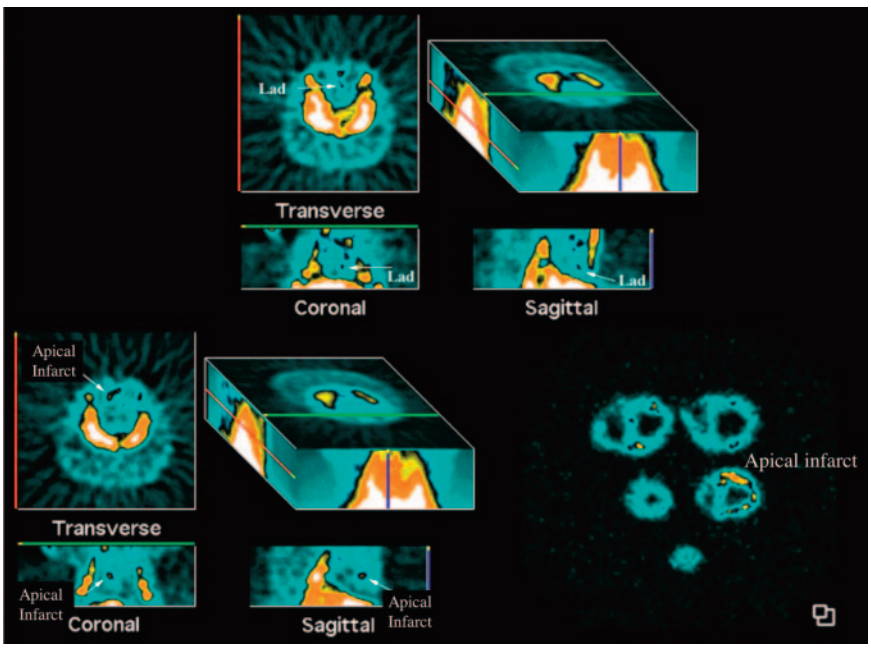

FIGURE 2. SPECT reconstructions (left) and ex vivo–imaged myocardial slices (bottom right). This animal had LAD injury and apical infarct. Focal uptake is seen in LAD and apex of left ventricle. Myocardial uptake was confirmed on ex vivo images.

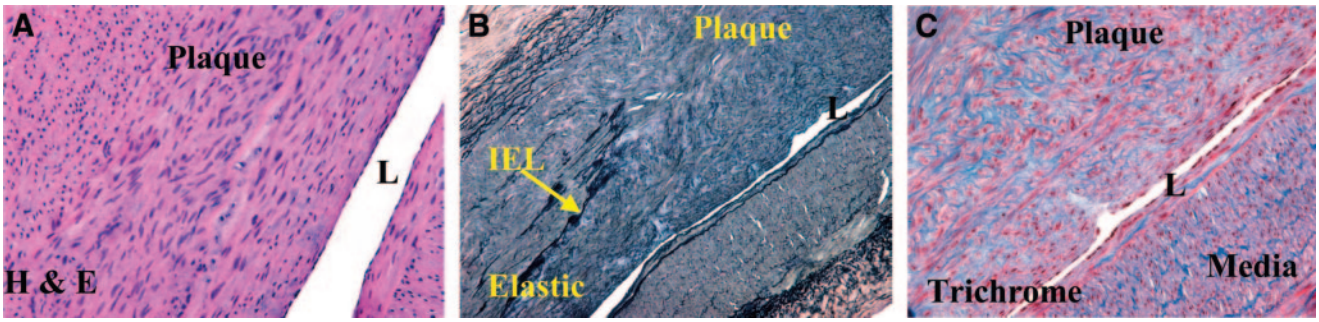

FIGURE 3. Photomicrographs of sections of injured coronary artery. Neointimal thickening is seen, comprising predominantly spindle-shaped cells characteristic of class II lesions. Sections are stained with hematoxylin and eosin (H & E) (A), elastic stain (B), and trichrome (C). Vessel was flattened for phosphor screen. IEL = internal elastic membrane; L = lumen.

DISCUSSION

This study was, to the best of our knowledge, the first to show that apoptosis of cells in the walls of the coronary arteries in a large-animal model of vascular injury can be visualized on in vivo SPECT using a conventional γ-camera. The diameters of the coronary arteries of humans and of large domestic swine are similar and below the resolution of γ-camera technology. Nuclear imaging techniques allow the detection of targets below the spatial resolution if the signal is sufficiently strong and the background low. The signal is detected as a small beacon or hot spot. Factors permitting the detection of small hot-spot targets include signal amplification through radiotracer design, a radiotracer with energy in a good range for in vivo imaging and high photon flux, a large number of target binding sites, and low nontarget binding. This study design met several of these criteria. Annexin V labeled with ^{99m}Tc has excellent imaging properties and has been shown to successfully image apoptosis of different organs in animal models (*5–11*). The radiolabeled tracer has rapid blood-pool clearance and low background activity. The process that was targeted—apoptosis of vascular smooth muscle cells—was highly active with many binding sites (>50% of cells) in this model.

Cells that could potentially undergo apoptosis in atherosclerotic plaque and bind with annexin V include macrophages, smooth muscle cells, and platelets. Our conclusion that the cells taking up the annexin V in this study are smooth muscle cells is based on serial sections showing positive staining for α-actin and negative staining for macrophages. No thrombi were seen on any of the vessel sections. Despite the absence of fresh thrombi, recent small, focal myocardial infarctions were seen in 6 experiments. All infarctions were in the territories of injured vessels. The most likely explanation for these findings is the occurrence of silent ischemia or necrosis from coronary spasm at the sites of vascular injury. Porcine coronary vascular endothelium is highly vasoactive, and porcine myocardium is susceptible to necrosis after relatively brief periods (10 min) of occlusion (*13*).

Apoptosis as a feature of human vascular pathology was observed and reported 10 y ago by several groups of investigators. Isner et al. examined human pathology specimens and found apoptosis in both atherosclerosis and restenosis, with a higher percentage of cells staining positively for apoptosis (terminal deoxynucleotidyl transferase–mediated dUTP nick-end labeling [TUNEL]) in restenosis specimens (*14*). Apoptosis was seen in both peripheral artery and

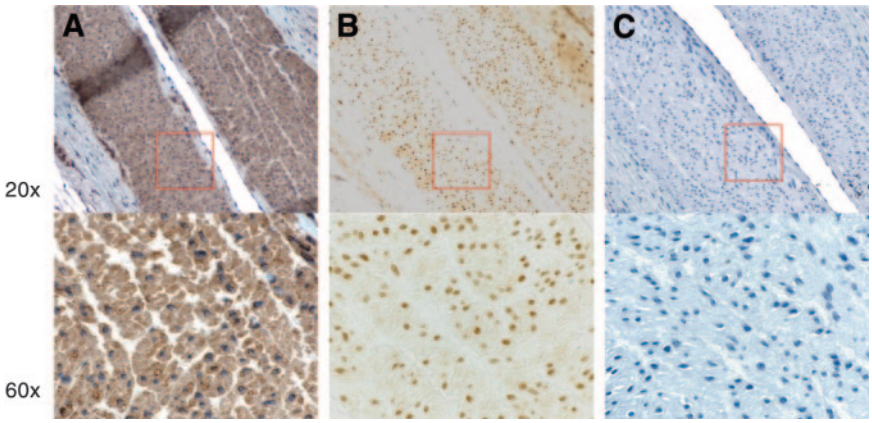

FIGURE 4. Photomicrographs of serial sections from injured scan-positive coronary vessel stained for α-actin (A), caspase-3 (B), and macrophages (C). Lesion cells staining positively for caspase-3 (B) were determined to be smooth muscle cells on the basis of brown cytoplasmic staining (A) and negative staining for macrophages (C).

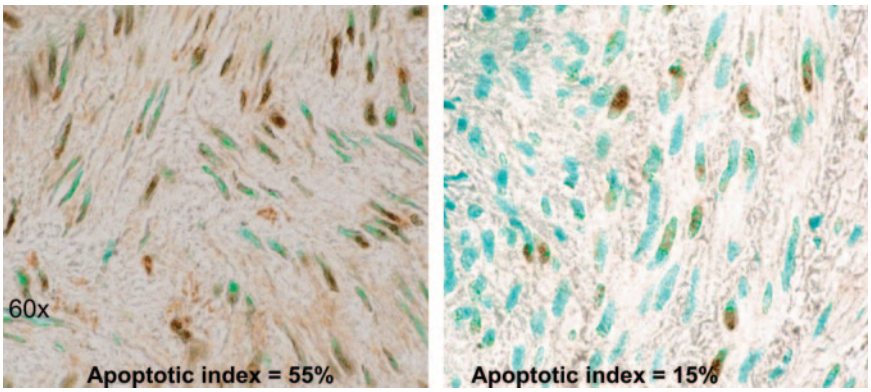

FIGURE 5. Photomicrographs of sections stained for caspase-3 (brown nuclear stain) with blue nuclear counterstain. On left is section from scan-positive injured vessel; on right, section from scan-negative injured vessel.

coronary artery lesions, with the highest percentage of apoptotic cells being 12%–18%. Bennett et al., in studying cultured vascular smooth muscle cells taken from human atherectomy tissue and from normal tissue from transplant donors, documented apoptosis in the cells from atherosclerotic tissue using time-lapse videomicroscopy, electron microscopy, and DNA fragmentation (*15*). Geng and Libby sectioned and stained human atheromata and removed cells for culture (*1*). They stained for both apoptosis (TUNEL) and cell type: smooth muscle cells (α-actin) and macrophages (CD68). They observed death rates of as high as 34%. The macrophages undergoing apoptosis localized in the lipid-rich core of lesions, whereas the smooth muscles undergoing apoptosis localized in the fibrotic portion of the atheroma. Several genes have been implicated in the death pathway in atherosclerotic lesions, including genes relating apoptosis with inflammation and low-density lipoprotein (*2,16–23*).

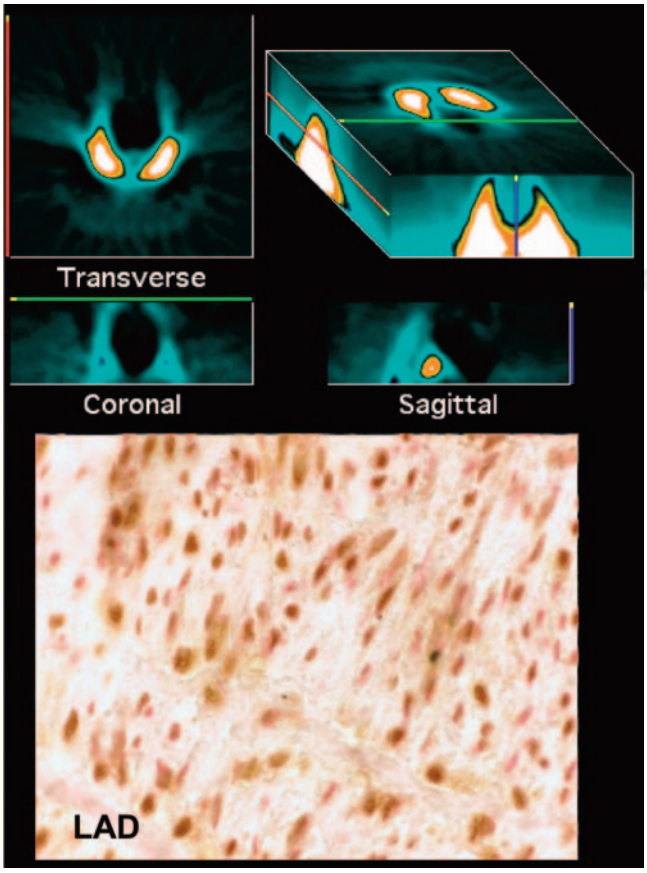

FIGURE 6. Animal injected with ^{99m}Tc-DTPA (control). SPECT reconstructions are on top, and photomicrograph of section from injured LAD is on bottom. No focal uptake of tracer is seen in region of heart. On immunohistochemical section, caspase chromagen is from a 3,3′-diaminobenzidine substrate kit (Vector Laboratories) and counterstain is nuclear fast red (Vector Laboratories). Section shows abundant brown nuclear and cytoplasmic staining corresponding to high rate of apoptosis in LAD.

Early work on the pathogenesis of atherosclerosis in swine was done by a group of investigators led by W.A. Thomas (*3,4,24–27*). Using a model of balloon injury of the abdominal aorta and a high-lipid diet in Yorkshire swine, they studied the population dynamics of smooth muscle cell proliferation and cell death. Using ^{3}H-labeled thymidine incorporation in cells, they compared the division pattern of smooth muscle cells in the animals with injury plus hypercholesterolemic diet to that in the animals with hypercholesterolemic diet alone. They found neointimal lesions of similar volumes in the 2 groups. The difference between the 2 groups was in the number of cell divisions and cell deaths. Compared with adjacent media, 4 times as many cells in the intima were synthesizing DNA and equal numbers of cells were undergoing cell death. These investigators also showed a significant positive correlation between the labeling indices of smooth muscle cells in lesions of the abdominal aorta and in the coronary arteries.

Although the role of vascular smooth muscle cell apoptosis in human atheromata is clearly established, its role in plaque vulnerability is probably not large. Data from human pathology specimens have determined that the cells undergoing apoptosis in unstable plaque are macrophages and not smooth muscle cells (*28*). Kolodgie et al. showed uptake of ^{99m}Tc-annexin on in vivo planar images of the abdominal aorta in a rabbit model of atherosclerosis (*11*). The tracer

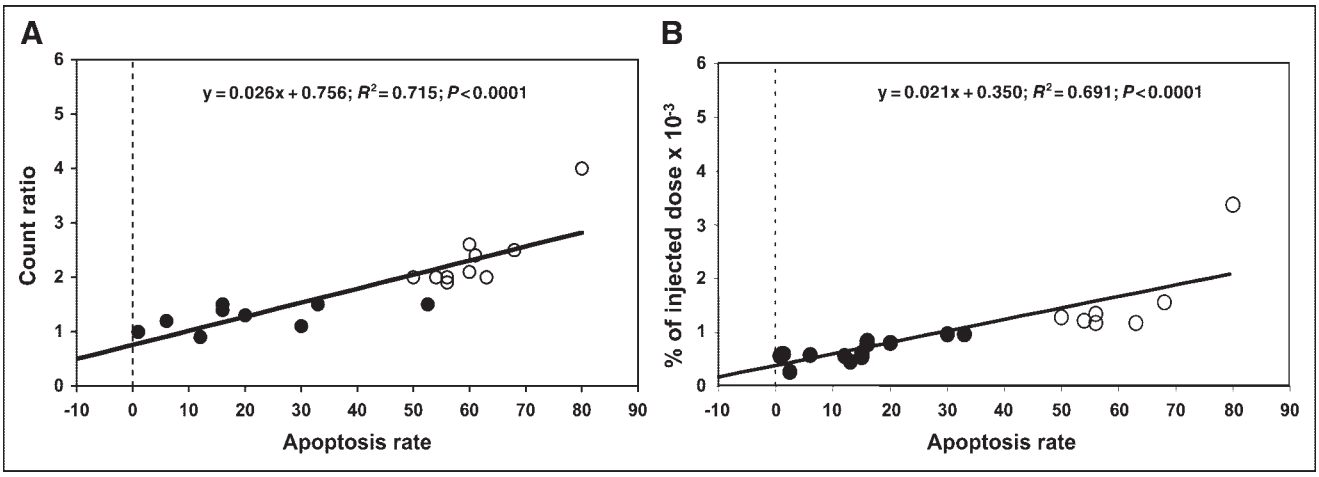

FIGURE 7. (A) Plot of count ratio (injured coronary artery to noninjured coronary artery) vs. apoptosis rate as determined from morphometric immunostaining. (B) Plot of tracer uptake vs. apoptosis rate. Closed circles represent experiments that did not show focal uptake in coronary arteries on in vivo SPECT; open circles represent experiments that did show focal uptake.

uptake corresponded to the location and severity (American Heart Association class) of the lesion and to the rate of macrophage death. The vascular injury model used in this study did not create the more advanced thin-cap fibroatheroma lesions. However, this study proved the concept that high rates of vascular cell death in the coronary arteries can be imaged in a model with coronary arteries similar in size to those of humans and with similar body mass indices and attenuating tissue.

This study had some limitations. Localizing focal uptake in the thorax to the coronary arteries without landmarks is difficult. Focal uptake of radiotracer in the myocardium in some animals further complicated scan interpretation. Correlation with the phosphor screen images of the coronary vessels and the ex vivo–imaged myocardial sections helped confirm the findings. Combined SPECT/CT with image fusion would have allowed precise localization of the hot spots to the vessels but was not available for this study.

CONCLUSION

The present study was, to the best of our knowledge, the first to provide proof of principle that noninvasive molecular imaging of a biologic feature of vulnerable plaque is feasible in coronary arteries.

ACKNOWLEDGMENTS

We thank Jane Freer in Rhode Island and Nicia Diaz in New York for their help in preparing the manuscript. This study was supported by grant 1RO1 HL68657-01 from the National Institutes of Health (Jagat Narula, principal investigator).

REFERENCES

1. Geng YJ, Libby P. Evidence for apoptosis in advanced human atheroma. *Am J Pathol.* 1995;147:251–266.
2. Jovinge S, Crisby M, Thyberg J, Nilsson J. DNA fragmentation and ultrastructural changes of degenerating cells in atherosclerotic lesions and smooth muscle cells exposed to oxidized LDL in vitro. *Arterioscler Thromb Vasc Biol.* 1997; 17:2225–2231.
3. Thomas WA, Scott RF, Florentin RA, Reiner JM, Lee KT. Population dynamics of arterial cells during atherogenesis. XI. Slowdown in multiplication and death rates of lesion smooth muscle cells in swine during the period 105–165 days after balloon endothelial cell denudation followed by a hyperlipidemic diet. *Exp Mol Pathol.* 1981;35:153–162.
4. Thomas WA, Kim DN, Lee KT, Reiner JM, Schmee J. Population dynamics of arterial cells during atherogenesis. XIII. Mitogenic and cytotoxic effects of a hyperlipidemic (HL) diet on cells in advanced lesions in the abdominal aortas of swine fed on HL diet for 270–345 days. *Exp Mol Pathol.* 1983;39:257–270.
5. Blankenberg FG, Katsikis PD, Tait J, et al. In vivo detection and imaging of phosphatidylserine expression during programmed cell death. *Proc Natl Acad Sci.* 1998;95:6349–6354.
6. Blankenberg FG, Katsikis PD, Tait J, Davis E, Naumovski L, Ohtsuki K. Imaging of apoptosis (programmed cell death) with ^{99m}Tc annexin V. *J Nucl Med.* 1999;40:184–191.
7. Blankenberg FG, Narula J, Strauss HW. In vivo detection of apoptotic cell death: a necessary measurement for evaluating therapy for myocarditis, ischemia and heart failure. *J Nucl Cardiol.* 1999;6:531–539.
8. Blankenberg FG, Strauss HW. Noninvasive strategies to image cardiovascular apoptosis. *Cardiol Clin.* 2001;19:165–172.
9. Blankenberg FG, Tait J, Blankenberg TA, Post AM, Strauss HW. Imaging macrophages and the apoptosis of granulocytes in a rodent model of subacute and chronic abscesses with radiolabeled monocyte chemotactic peptide-1 and annexin V. *Eur J Nucl Med.* 2001;28:1384–1393.
10. Hofstra L, Liem IH, Dumont EA, Boersma HH, vanHeerde WL, Doevendans PA. Visualization of cell death in vivo in patients with acute myocardial infarction. *Lancet.* 2000;356:209–212.
11. Kolodgie FD, Petrov A, Virmani R, et al. Targeting of apoptotic macrophages and experimental atheroma with radiolabeled annexin V: a technique with potential for noninvasive imaging of vulnerable plaque. *Circulation.* 2003;108: 3134–3139.
12. Thomas WA, Reiner JM, Florentin RA, Lee KT, Lee WM. Population dynamics of arterial cells during atherogenesis V: cell proliferation and cell death during initial 3 months in atherosclerotic lesions induced in swine by hypercholesterolemic diet and initial trauma. *Exp Mol Pathol.* 1976;24:360–374.
13. Woolf N. Animal models of myocardial ischaemia. *J Clin Pathol Suppl (R Coll Pathol).* 1977;11:53–58.
14. Isner JM, Kearney M, Bortman S, Passeri J. Apoptosis in human atherosclerosis and restenosis. *Circulation.* 1995;91:2703–2711.
15. Bennett MR, Evan GI, Schwartz SM. Apoptosis of human vascular smooth muscle cells derived from normal vessels and coronary atherosclerotic plaques. *J Clin Invest.* 1995;95:2266–2274.
16. Bennett MR, Littlewood TD, Schwartz SM, Weissberg PL. Increased sensitivity

of human vascular smooth muscle cells from atherosclerotic plaques to p53-mediated apoptosis. *Circ Res.* 1997;81:591–599.
17. Bai H, Pollman MJ, Inishi Y, Gibbons GH. Regulation of vascular smooth muscle cell apoptosis: modulation of Bad by a phosphatidylinositol 3-kinase-dependent pathway. *Circ Res.* 1999;85:229–237.
18. Bjorkerud S, Bjorkerud B. Apoptosis is abundant in human atherosclerotic lesions, especially in inflammatory cells (macrophages and T cells), and may contribute to the accumulation of gruel and plaque instability. *Am J Pathol.* 1996;149:367–380.
19. Hasdai D, Sangiorgi G, Spagnoli LG, et al. Coronary artery apoptosis in experimental hypercholesterolemia. *Atherosclerosis.* 1999;142:317–325.
20. Minamino T, Yoshida T, Tateno K, et al. Ras induces vascular smooth muscle cell senescence and inflammation in human atherosclerosis. *Circulation.* 2003; 108:2264–2269.
21. Seshiah PN, Kereiakes DJ, Vasudevan SS, et al. Activated monocytes induce smooth muscle cell death: role of macrophage colony-stimulating factor and cell contact. *Circulation.* 2002;105:174–180.
22. Geng YJ, Henderson LE, Levesque EB, Muszynski M, Libby P. Fas is expressed in human atherosclerotic intima and promotes apoptosis of cytokine-primed human vascular smooth muscle cells. *Arterioscler Thromb Vasc Biol.* 1997;17: 2200–2208.
23. Schaub FJ, Han DKM, Liles WC, et al. Fas/FADD-mediated activation of a specific program of inflammatory gene expression in vascular smooth muscle cells. *Nat Med.* 2000;6:790–796.
24. Scott RF, Reidy MA, Kim DN, Schmee J, Thomas WA. Intimal cell mass-derived atherosclerotic lesions in the abdominal aorta of hyperlipidemic swine. Part 2. Investigation of endothelial cell changes and leukocyte adherence associated with early smooth muscle cell proliferative activity. *Atherosclerosis.* 1986; 62:27–38.
25. Scott RF, Kim DN, Schmee J, Thomas WA. Atherosclerotic lesions in coronary arteries of hyperlipidemic swine. Part 2. Endothelial cell kinetics and leukocyte adherence associated with early lesions. *Atherosclerosis.* 1986; 62:1–10.
26. Kim DN, Imai H, Schmee J, Lee KT, Thomas WA. Intimal cell mass-derived atherosclerotic lesions in the abdominal aorta of hyperlipidemic swine. Part 1. Cell of origin, cell divisions and cell losses in first 90 days on diet. *Atherosclerosis.* 1995;56:169–188.
27. Thomas WA, Kim DN, Geourzoung SM, Schmee J, Lee KT. Association of plasma intermediate density lipoproteins with atherogenic intimal proliferative activity in abdominal aortas of hyperlipidemic swine. *Atherosclerosis.* 1985;58: 223–241.
28. Kolodgie FD, Narula J, Burke AP, et al. Localization of apoptotic macrophages at the site of plaque rupture in sudden coronary death. *Am J Pathol.* 2000;157: 1259–1268.